DOI: 10.1002/chem.200600843

Unprecedented Polymerization of Trimethylene Carbonate Initiated by a Samarium Borohydride Complex: Mechanistic Insights and Copolymerization with ε-Caprolactone

Isabelle Palard,[a] Michèle Schappacher,[a] Benjamine Belloncle,[a] Alain Soum,[a] and Sophie M. Guillaume*[a, b]

Abstract: Poly(trimethylene carbonate) (PTMC) was synthesized through ring-opening polymerization by using a rare-earth borohydride initiator, [Sm-$(BH_4)_3(thf)_3$]. This initiator shows a high activity to give high-molar-mass PTMCs with molar-mass distributions ranging from 1.2 to 1.4, and with a regular structure void of ether linkages. The polymers were characterized by ^{1}H and ^{13}C NMR spectroscopy, ^{1}H-^{1}H COSY, ^{1}H-^{13}C HMQC NMR spectroscopy, size-exclusion chromatography (SEC), viscosimetry, and MALDI-TOF MS analyses. A coordination-insertion mechanism was established based on detailed NMR characterizations, especially of the polymer chain end-functions. The monomer initially coordinates the samarium to give [$Sm(BH_4)_3$-$(tmc)_3$], **1**. The monomer then opens up through cleavage of the cyclic ester oxygen−acyl bond and inserts into the Sm−HBH_3 bond resulting in an alkoxide complex, [$Sm\{O(CH_2)_3OC(O)$-$HBH_3\}_3$], **2**, or [$Sm\{O(CH_2)_3OC(O)$-$H\}_3$], **2′**, which then propagates the polymerization of TMC to give the active polymer [$Sm(\{O(CH_2)_3OC(O)\}_n$-$O(CH_2)_3OC(O)HBH_3)_3$], **3** or [$Sm(O$-$(CH_2)_3OC(O)\{O(CH_2)_3OC(O)\}_nO$-$(CH_2)_3OC(O)H)_3$], **3′**. Finally, acidic hydrolysis of **3** or **3′** gives HO-$(CH_2)_3OC(O)[O(CH_2)_3OC(O)]_nO$-$(CH_2)_3OC(O)H$, **4**. This novel α-hydroxy,ω-formatetelechelic PTMC represents the first example of a formate-terminated polycarbonate. TMC and ε-caprolactone (CL) were copolymerized to afford both random PTMC-*co*-PCL and block PTMC-*b*-PCL copolymers that were characterized by ^{1}H NMR spectroscopy, SEC, and differential scanning calorimetry (DSC). The structure of the block copolymers depends on the order of addition of monomers: if CL is introduced first, dihydroxytelechelic HO-PTMC-*b*-PCL-OH polymers are formed, whereas introduction of TMC first or simultaneous addition of comonomers leads to hydroxyformate-telechelic HC(O)O-PTMC-*b*-PCL-OH analogues.

Keywords: block copolymers · borohydride · carbonates · rare earth metals · ring-opening polymerization

Introduction

Ring-opening polymerization (ROP) of cyclic esters, namely lactones, diesters, and carbonates, initiated by rare-earth derivatives has attracted growing attention in the past two decades.[1–7] Aliphatic polyesters and polycarbonates, as well as their copolymers, are indeed highly attractive as biomaterials for their biocompatibility and bioresorbability. They are widely used in drug-delivery systems or in tissue engineering.[4,5,8,9] Regarding rare-earth-initiated polymerizations, most of the literature deals with lactones, especially poly(ε-caprolactone) (PCL) and polylactide (PLA), which have many applications as homopolymers as well as copolymers in biomedical and pharmaceutical domains.[1–9]

As part of our ongoing research on the ROP of cyclic esters,[10–13] after understanding and mastering the polymeri-

[a] Dr. I. Palard, M. Schappacher, B. Belloncle, Prof. A. Soum, Dr. S. M. Guillaume
Laboratoire de Chimie des Polymères Organiques
CNRS-ENSCPB-Université Bordeaux 1
ENSCPB, 16 Avenue Pey-Berland, 33607 Pessac Cedex (France)
Fax: (+33) 5-4000-8487
E-mail: guillaume@enscpb.fr

[b] Dr. S. M. Guillaume
Current address: Unité Sciences Chimiques de Rennes
CNRS UMR6226 – Université de Rennes 1
Campus de Beaulieu
Laboratoire Catalyse et Organométalliques
35042 Rennes Cedex (France)
Fax : (+33) 2-2323-6939
E-mail: sophie.guillaume@univ-rennes1.fr

Supporting information for this article is available on the WWW under http://www.chemistry.org or from the author.

zation of ε-caprolactone (CL) initiated by rare-earth borohydride complexes,[14–17] we now investigate the polymerization of carbonates, exemplified by trimethylene carbonate (1,3-dioxan-2-one, TMC) by using $[Sm(BH_4)_3(thf)_3]$ as initiator. Only a few reports mention the homopolymerization of carbonate using similar rare-earth initiating species, essentially of TMC,[18–23] and also of dimethyl- or ethylene-substituted carbonates.[21,24–30] Poly(trimethylene carbonate (PTMC) exhibiting quite high molar-mass distributions (1.4–2.45) have been synthesized from homoleptic trivalent rare-earth complexes, such as the cyclopentadienyl $[Ln(\eta\text{-}C_5H_5)_3]$ (Ln = Ce, Pr, Sm, Gd, Er), the guanidinate $[Ln\{R_2NC(NR')_2\}_3]$ (R = *i*Pr, Ph, Cy; R′ = $(CH_2)_5$, *i*Pr, Ph; Ln = Nd, Sm, Yb), the alkoxide $Ln(OAr)_3$ (Ar = 2,6-di-tert-butyl-4-methylphenolate; Ln = Sc, La), or the halides LnX_3 (Ln = La, Nd, Sm, Gd, Dy, Yb; X = Cl, Br), at temperatures ranging from 0 to 80 °C. In the present paper, we report the first polymerization of a carbonate, TMC, by using a rare-earth borohydride complex, $[Sm(BH_4)_3(thf)_3]$, with a particular emphasis on the polymerization mechanism. Comparisons with the related CL polymerization initiated by $[Ln(BH_4)_3(thf)_3]$ (Ln = La, Nd, Sm) are also drawn.

Knowledge and control of the homopolymerization processes of both TMC and CL subsequently allow their copolymerization to be investigated to access novel macromolecular architectures. Although PCL is a semicrystalline polymer with a glass transition temperature (T_g) of −66 °C, PTMC (T_g = −15 °C) is rather amorphous.[31] Furthermore, because ester bonds are more sensitive to hydrolysis than carbonates, which are almost totally resistant, PCL degrades faster than PTMC.[4,5,9] Thus, copolymerization of TMC and CL enables tuning of the physical properties (e.g., morphology, crystallinity) and the degradation behavior of the resulting material, and thereby facilitates access to tailor-made biopolymers. Optimized tissue affinity, drug compatibility, and drug release can, therefore, be monitored within PTMC–PCL copolymers.[32] In addition, copolymers of CL can exhibit a wide range of elasticity and softness, two features that might be required simultaneously within a biomaterial such as a guide for in vivo nerve reconstruction.[31,33] Some PTMC–PCL copolymers have been synthesized from various rare-earth halide (LnX_3/epoxide or isopropoxide) or alkoxide ("$Ln(OiPr)_3$") (Ln = Y, La); $Sc(OAr)_3$ (Ar = 2,6-di-*tert*-butyl-4-methylphenolate); (EA)Ln(O*i*Pr) (EA = diethyl acetoacetate, Ln = Y, Nd)) initiators.[20,22,23,31–35] Other studies involve different d transition-metal complexes, such as tin, bismuth, zinc, or aluminum.[36] In addition, other poly(carbonate)-PCL[21,25–29] and PTMC–PLA[37–39] have been obtained from other rare-earth initiators. Thus, in addition to the TMC homopolymerization, we also describe the synthesis of both random and block PTMC–PCL copolymers initiated by $[Sm(BH_4)_3(thf)_3]$. For these copolymers, the chain end-functional groups depend on the order of monomer addition.

Results and Discussion

Homopolymerization of TMC initiated by $[Sm(BH_4)_3(thf)_3]$: Rare-earth trisborohydride complexes, such as the samarium species $[Sm(BH_4)_3(thf)_3]$ used in the present study, are easily prepared from the corresponding rare-earth trichloride, according to a now well-established procedure.[40,41] In addition, they are structurally well characterized and exhibit a monomeric structure $[Ln\{(\mu_2\text{-}H)_3BH\}_2(\mu_2\text{-}H)_2BH_2(thf)_3]$, as determined by X-rays analysis.[42] Although the advantage of using such borohydride-substituted rare-earth derivatives (as opposed to the more common chlorides, to which they are isosteric, yet not isoelectronic) was demonstrated initially with the growth of neodymium borohydride organometallic chemistry,[40,41,43,44] the impact of the borohydride functional group in ROP is indeed now confirmed. Indeed, an unusual reactivity was unveiled during the polymerization of CL, based on the advantage offered by the intrinsic reactivity of the BH_4^- ligand.[14–17] In this case, direct synthesis of α,ω-dihydroxytelechelic PCL was achieved upon the in situ reaction of the BH_3 end unit with the adjacent carbonyl on the active polymer chain, resulting ultimately in an unforeseen second hydroxyl end group on the final PCL. Consequently, a similar unusual behavior was expected regarding the polymerization of TMC.

General data: The homoleptic trivalent rare-earth borohydride complex $[Sm(BH_4)_3(thf)_3]$ initiated the ring-opening polymerization of TMC (Table 1). The reactions performed in CH_2Cl_2 or THF over 1–4 h at 21 °C give high yields of PTMC of molar mass ranging from 2000 to 27000 g mol^{-1}

Table 1. Polymerization of TMC initiated by $[Sm(BH_4)_3(thf)_3]$.

$[BH_4]_0$[a] [mmol L^{-1}]	$[TMC]_0$ [mmol L^{-1}]	$[TMC]_0/[BH_4]_0$	Solvent	Reaction time [min]	Monomer conv.[b] [%]	$\bar{M}_{n(theo)}$[c] [g mol^{-1}]	$\bar{M}_{n(SEC)}$[d] [g mol^{-1}]	$\bar{M}_w/\bar{M}_n$[e]
64.8	1225	19	CH_2Cl_2	60	95	1850	2000	1.18
60.7	1225	20	THF	60	90	1850	2100	1.40
32.8	1225	37	CH_2Cl_2	60	95	3600	2350	1.24
18.2	1225	67	CH_2Cl_2	90	94	6400	7350	1.31
18.2	1225	67	THF	60	95	6500	5900	1.37
14.2	1225	86	THF	90	81	7100	5400	1.31
14.6	2450	168	THF	180	84	14400	13500	1.39
12.8	2450	191	THF	240	97	18900	17050	1.40
10.2	2450	240	THF	240	86	21050	19150	1.35
7.65	2450	320	THF	240	79	25800	24100	1.23
7.1	2450	345	THF	240	74	26050	27050	1.32

[a] $[BH_4]_0 = 3[Sm(BH_4)_3(thf)_3]_0$. [b] Determined by ^{1}H NMR analysis. [c] Calculated from $[TMC]_0/[BH_4]_0 \times 102 \times$ monomer conversion. [d] Determined by SEC using the correction coefficient X and $\bar{M}_{n(SEC)} = \bar{M}_{n(SEC\ raw\ data)} \times X$ (see Experimental Section). [e] Molar-mass distribution calculated from SEC chromatogram traces.

with a moderate broadening of the molar-mass distribution (1.2–1.4). The monomer conversions, which depend on the reaction time and on both the monomer and the initiator concentrations, range from 74 to 97%, in agreement with an equilibrated polymerization observed previously.[36c]

Theoretical molar masses $\bar{M}_{n(theo)}$ were calculated from the initial concentration in samarium initiator ($[Sm(BH_4)_3(thf)_3]_0$) on the basis of three active sites per metal available for polymerization. Number-average molar-mass values of PTMC derived from size-exclusion chromatography (SEC) measurements ($\bar{M}_{n(SEC\ raw\ data)}$) were corrected, to reflect actual values, by multiplication with a factor X determined from measurements of the molar mass using several techniques, especially MALDI-TOF and viscosimetry (see Experimental Section). Indeed, calibration of SEC elution curves with commercial polystyrene standards (as performed usually) overestimates the real molar mass of aliphatic polyesters.[11,36f,h] The corrected molar-mass values $\bar{M}_{n(SEC)}$ ($=\bar{M}_{n(SEC\ raw\ data)} \times X$) are in quite good agreement with the calculated values $\bar{M}_{n(theo)}$ and increase linearly as $[TMC]_0/[BH_4]_0$ ratios increase (Figure 1), while the molar-mass distributions

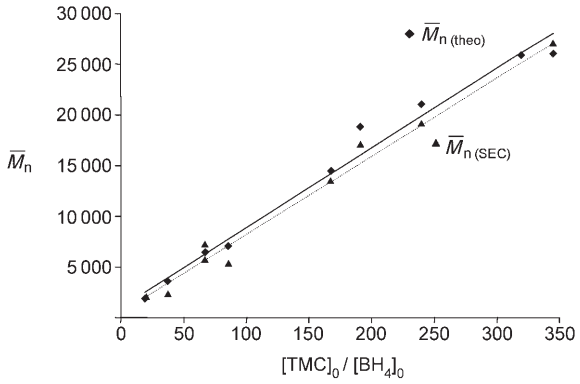

Figure 1. Variations of the theoretical ($\bar{M}_{n(theo)}$) and SEC ($\bar{M}_{n(SEC)}$) molar-mass values versus $[TMC]_0/[BH_4]_0$ for the polymerization of TMC initiated by $[Sm(BH_4)_3(thf)_3]$ (Table 1).

remain quite constant and relatively low (1.2–1.4), regardless of the initial concentration of $[Sm(BH_4)_3(thf)_3]$.[45] These features suggest that polymerization takes place without significant transfer reactions and that the occurrence of inter- and intramolecular side reactions (reshuffling and backbiting) can be neglected during the propagation. This is further confirmed by the absence of any detectable low-molar-mass side products in the SEC trace of a crude polymer (polymer before precipitation). Therefore, the use of the samarium borohydride initiator seems to allow a better control of the TMC polymerization reaction than that reported previously for other rare-earth complexes.[45]

^{1}H and ^{13}C NMR analyses of the PTMCs reveal two distinct chain ends, one hydroxy and one formate, each being identified by typical signals that are indeed correlated in the ^{1}H-^{13}C HMQC spectrum [HOCH_2- at $\delta 1_{Ha}=3.71$ ppm (triplet) and $\delta 13_{C1}=59.9$ ppm; -$(CH_2)_3$OC(O)H at $\delta 1_{Hj}=8.03$ ppm (singlet) and $\delta 13_{C12}=161.8$ ppm] (Figures 2–4).

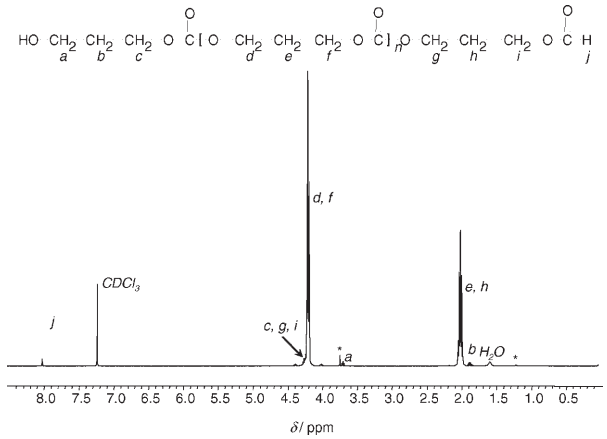

Figure 2. ^{1}H NMR spectrum of PTMC in $CDCl_3$ (Table 1, $[TMC]_0/[BH_4]_0=168$; $\bar{M}_{n(SEC)}=13\,500$ g mol^{-1}).

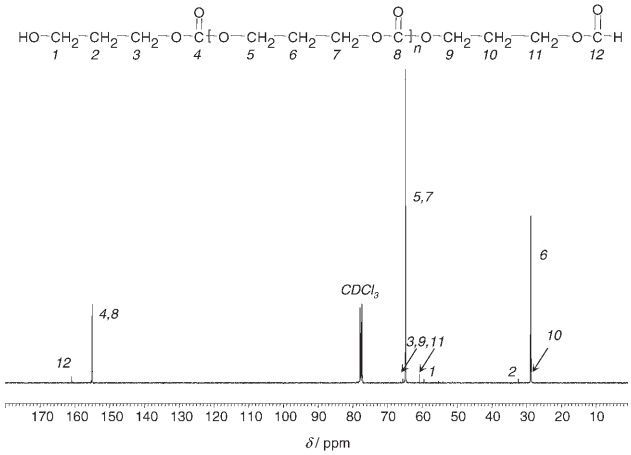

Figure 3. ^{13}C NMR spectrum of PTMC in $CDCl_3$ (Table 1, $[TMC]_0/[BH_4]_0=168$; $\bar{M}_{n(SEC)}=13\,500$ g mol^{-1}).

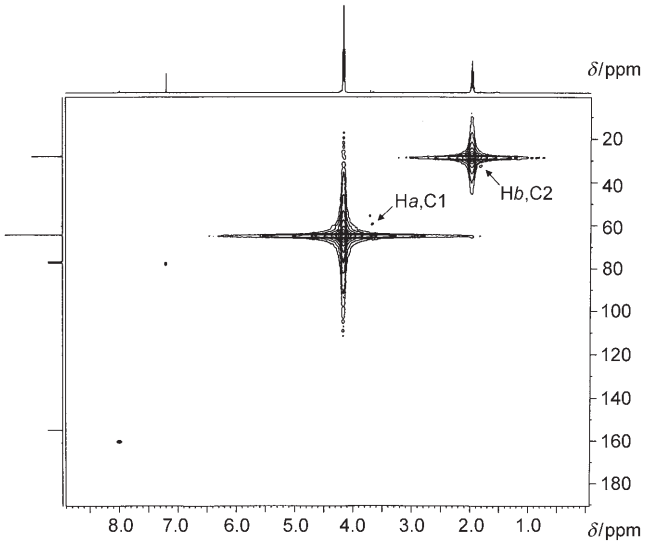

Figure 4. ^{1}H-^{13}C HMQC NMR spectrum of PTMC in $CDCl_3$ (Table 1, $[TMC]_0/[BH_4]_0=168$; $\bar{M}_{n(SEC)}=13\,500$ g mol^{-1}).

The PTMC signals were assigned based on ^{1}H-^{13}C HMQC and two-dimensional ^{1}H-^{1}H COSY spectra (Figures 4 and 5). Both sets of signals corresponding to each chain end (hydroxyl: H*a*,H*b*,H*c*-C*1*,C*2*,C*3* and formate: H*g*,H*h*,H*i*-C*9*,C*10*,C*11*, respectively), could be differentiated from the coupling observed between the HOCH_2 hydroxymethylene triplet ($\delta 1_{Ha}=3.71$ ppm) and the HOCH$_2$CH_2CH$_2$OC(O) methylene quintuplet ($\delta 1_{Hb}=1.89$ ppm), the latter being also coupled to the carbonatemethylene triplet HOCH$_2$CH$_2$CH_2OC(O) ($\delta 1_{Hc}=4.27$ ppm). Although the whole hydroxy end-group HO(CH$_2$)$_3$OC(O)$-$ is thus observed unambiguously in these spectra, all of the formate chain end signals $-$CH$_2$CH$_2$CH$_2$OC(O)H cannot be identified clearly because their overlap with the main chain signals does not allow resolved cross-peaks to be observed. Notably, the decarboxylation of the carbonate does not take place during polymerization, as highlighted in the NMR spectra of PTMCs by the absence of peaks at $\delta 1_H=3.3$–3.1 ppm and $\delta 13_C=66.5$–67.7 ppm, typical of ether units that are formed generally as defects in the polymer structure.[18,28,46]

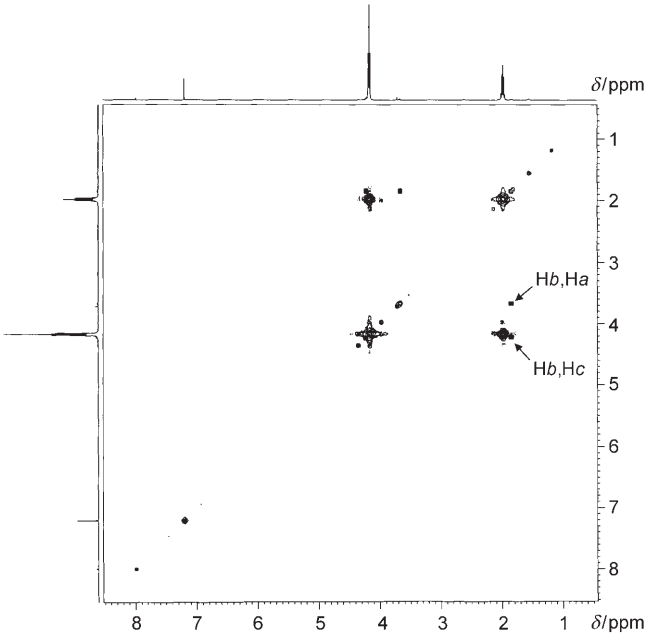

Figure 5. ^{1}H-^{1}H COSY spectrum of PTMC in $CDCl_3$ (Table 1, $[TMC]_0/[BH_4]_0=168$; $\bar{M}_{n(SEC)}=13\,500$ g mol^{-1}).

MALDI-TOF mass spectrometry analyses of low-molar-mass PTMC samples ($\bar{M}_n<5000$ g mol^{-1}) show signals of a main envelop corresponding to HO(CH$_2$)$_3$OC(O)-PTMC-O-(CH$_2$)$_3$OC(O)H, **4** (see below). Decarboxylated ($m/z=44$) analogous chains, resulting apparently from the MALDI experimental analysis conditions as they are never observed in NMR spectra, are also detected along with chains with $m/z=28$ (C(O)) and $m/z=74$ (O(CH$_2$)$_3$O), most likely corresponding to cyclic polymers. This suggests the presence of some side products, although in limited a amount as they are not detected in SEC analysis, resulting from intramolecular (backbiting) side reactions.

Comparison with the polymerization of CL initiated by the same initiator [Sm(BH$_4$)$_3$(thf)$_3$] indicates that molar-mass and molar-mass distribution values of PTMC are within the same range as those of PCL ($3500<\bar{M}_n<40\,000$ g mol^{-1}; $1.1<\bar{M}_w/\bar{M}_n<1.5$), but that the TMC polymerization is slower (quantitative CL conversion in 10 min versus 95 % TMC conversion in 60 min).[15,16,17] Although both PCL and PTMC are telechelic, PCL is dihydroxy-terminated and TMC polymers exhibit two different end-functionalities; hydroxy and formate. This eventually suggests distinct, active PTMC- and PCL-chain end-functions, resulting ultimately in polymers that are not similarly end-functionalized. A different mechanism for each monomer type, and most likely a different $(BH_4)^-$ reactivity during the polymerization process, can thus be supposed.

Mechanistic insights: To elucidate the formation of α-hydroxy,ω-formatetelechelic PTMC, the equimolar addition of TMC to [Sm(BH$_4$)$_3$(thf)$_3$] was first monitored stepwise by in situ NMR spectroscopy (Scheme 1). The spectrum (Figure 6) reveals the displacement of the three THF molecules from the samarium center; indeed, because Sm^{III} is paramagnetic ([Xe]4f^{5}5d^{0}6s^0), coordinated THF signals appear at lower field (4.23; 2.22 ppm) relative to free (displaced) THF signals (3.81; 1.94 ppm). However, the resulting product precipitates from the CD_2Cl_2 solution, thus precluding further solution characterization. IR analysis of this solid exhibits typical signals for the expected metal–BH$_4$ tridentate and bidentate ligands within the region 2425–2165 cm^{-1}.[47] Indeed, a bonding similar to that observed for the THF analogue [Sm{(μ$_2$-H)$_3$BH}$_2${(μ$_2$-H)$_2$BH$_2$}(thf)$_3$] is expected.[42,47] In this TMC adduct, the carbonate would be coordinated to the samarium through the carbonyl oxygen atom in agreement with the strong Lewis acidic character of rare-earth metals and with the basic character of cyclic esters.[20,48,49] To further confirm the exchange of THF with TMC, we used a nonpolymerizable carbonate, diethylcarbonate (Et$_2$CO$_3$=DEC; Scheme 2) as a model. THF is indeed displaced similarly and the resulting product [Sm(BH$_4$)$_3$(dec)$_3$] remains soluble, allowing its solution characterization by NMR spectroscopy (Figure 6). The slight downfield displacement of DEC from the free molecule

$$[Sm(BH_4)_3(thf)_3] + 3\ TMC \xrightarrow[21^\circ C]{CD_2Cl_2} \underset{\mathbf{1}}{[Sm(BH_4)_3(tmc)_3]} + 3\ THF$$

Scheme 1. Stoichiometric reaction of TMC with [Sm(BH$_4$)$_3$(thf)$_3$].

$$[Sm(BH_4)_3(thf)_3] + 3\ CH_3CH_2OC(O)OCH_2CH_3 \xrightarrow[21^\circ C]{CD_2Cl_2} [Sm(BH_4)_3(dec)_3] + 3\ THF$$
DEC

Scheme 2. Stoichiometric reaction of DEC with [Sm(BH$_4$)$_3$(thf)$_3$].

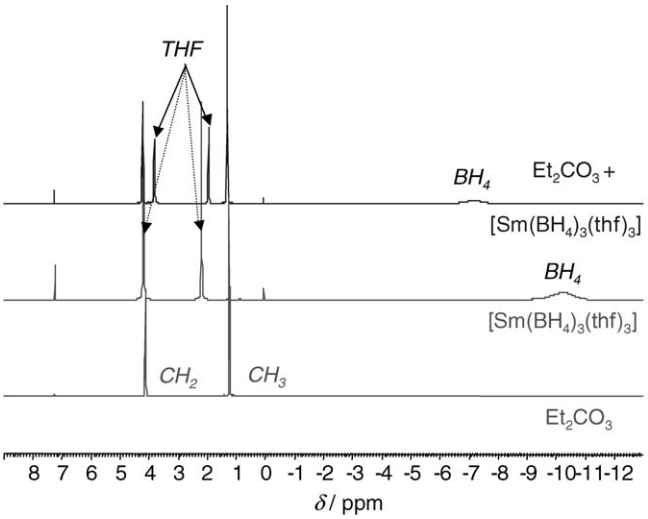

Figure 6. ^{1}H NMR spectra showing the formation of $[Sm(BH_4)_3(dec)_3]$ from the reaction of $[Sm(BH_4)_3(thf)_3]$ with DEC.

(4.12; 1.24 ppm) to Sm-coordinated DEC (4.22; 1.31 ppm) concomitant with the release of THF confirms the THF/DEC exchange. These data thus support that the first step of the initiation process of the polymerization of TMC involves substitution of the coordinated THF of $[Sm(BH_4)_3(thf)_3]$ by the first three incoming carbonate molecules to give $[Sm(BH_4)_3(tmc)_3]$, **1** (Scheme 1).

Once $[Sm(BH_4)_3(tmc)_3]$, **1**, is formed, the second step of the initiation process involves the nucleophilic attack of $[Sm(BH_4)_3(tmc)_3]$ on the carbon atom of the TMC carbonyl function, followed by the carbonate insertion into the Sm–HBH_3 bond with either an oxygen–acyl or oxygen–alkyl bond cleavage. Each type of monomer ring-opening would generate specific chain ends exhibiting characteristic NMR signals. Breaking of an OC(O)–O bond would induce the formation of hydroxyl and formate end-functions (Scheme 3a), whereas rupture of an OC(O)O–CH_2 bond would lead to HOC(O)O– and a –CH_2CH_3 end groups (Scheme 3b). NMR analyses of the polymer samples show the absence of the (representative and distinct) signals corresponding to a carbonate/alkyl species at 4.2 ($HOC(O)OCH_2$) and 1.0 ppm ($CH_2CH_2CH_3$) in the ^{1}H spectra and at 22.0 ($CH_2CH_2CH_3$) and 9.7 ppm ($CH_2CH_2CH_3$) in the ^{13}C spectra (Figures 2 and 3, Scheme 3b). Indeed, apart from the main polymer-chain peaks, the spectra exhibit signals at 3.71/59.9 and 8.03/161.8 ppm corresponding to the $HOCH_2$ and $OC(O)H$ protons and carbons, respectively, generated upon a TMC oxygen–acyl scission (Figures 2 and 3). Combining all these results thus suggests that the TMC most likely opens up through rupture of an oxygen–acyl bond to give the samarium alkoxide species $[Sm\{O(CH_2)_3OC(O)HBH_3\}_3]$, **2**, as illustrated in Scheme 3a.

The terminal carbonyl function of **2** might then undergo reduction by the adjacent HBH_3 group, as observed previously during the initiation process of ε-caprolactone by similarly using $[Sm(BH_4)_3(thf)_3]$.[14,16] As illustrated in Scheme 4b, reduction of the C(O) in the α-position of the HBH_3 end-function would lead to the formation of an alkoxyborane species $[Sm\{O(CH_2)_3O(CH_2)(OBH_2)\}_3]$ that, upon final hydrolysis, would give a dihydroxytelechelic PTMC.[14,16] The absence of C(O) reduction would result in

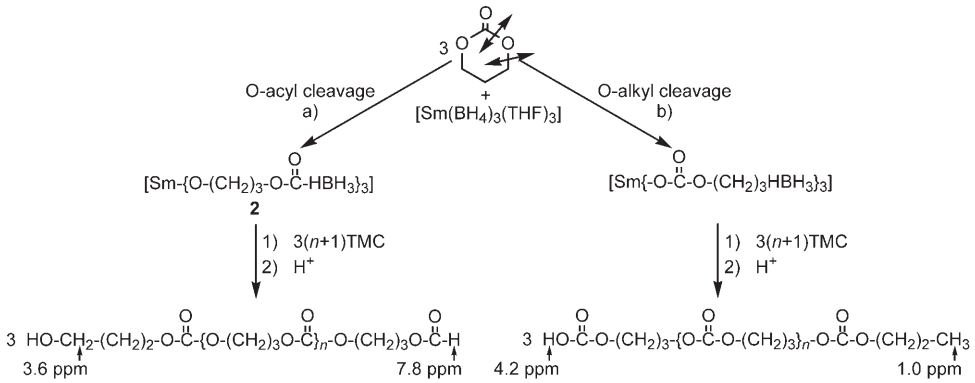

Scheme 3. Potential TMC ring-openings during the polymerization initiated by $[Sm(BH_4)_3(thf)_3]$.

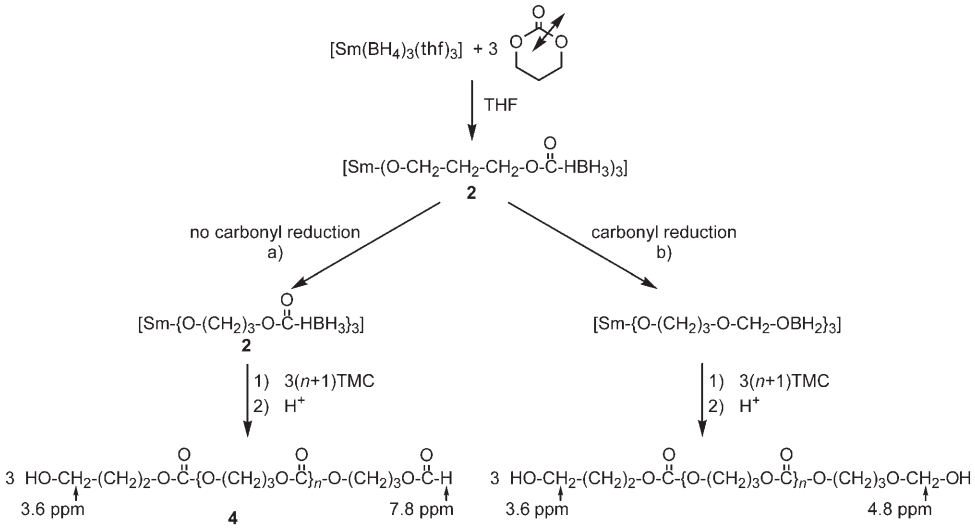

Scheme 4. Potential HBH_3^- reactivity during the polymerization initiated by $[Sm(BH_4)_3(thf)_3]$.

a samarium alkoxide terminated by a formate-BH_3 group, $[Sm\{O(CH_2)_3OC(O)HBH_3\}_3]$, **2**, that, after the ultimate hydrolytic cleavage of the active Sm–O bond along with elimination of the borane adduct (BH_3·THF), would generate an α-hydroxy,ω-formatetelechelic PTMC, **4** (Scheme 4a). Because an additional type of polymer chain end (formate) is observed in the NMR spectra along with the hydroxyl end, the reduction is thus presumed not to occur. In addition, the significant peaks for a O-$(CH_2)_3OCH_2OH$ terminated polymer are not observed in the ^1H spectra at 4.8 (OCH_2OH) or 3.4 ppm (CH_2OCH_2OH), nor in the ^{13}C spectra at 87.4 ppm (OCH_2OH). Further evidence of the nonreduction of the TMC carbonyl group was sought. Firstly, because no "OC(O)–HBH_3" model is available, BH_3·THF was placed in the presence of methyl formate ($CH_3OC(O)H$), which remains unreacted even in the presence of a large excess (up to ten equivalents) of borane (the intensity of the OC(O)*H* signal at 8.05 ppm remains constant relative to that of the BH_3·THF quadruplet (0.9 ppm), which grows proportionally to the amount added). This suggests that the BH_3 group may not react with the adjacent C=O in $[Sm\{O(CH_2)_3OC(O)HBH_3\}_3]$, **2** (Scheme 4a). Additional evidence was gained upon monitoring, by in situ ^1H NMR spectroscopy, the reaction of TMC with $[La(BH_4)_3(thf)_3]$, a diamagnetic ($[Xe]5d^06s^0$) rare-earth complex analogous to the (paramagnetic) samarium initiator. As observed previously from similar comparative experiments, the narrower signals recorded with this active lanthanum species allow a better understanding of the spectra than those obtained with the samarium initiator.[14] In addition, monitoring the evolution of the active species should allow visualization of the eventual carbonyl reduction. The ^1H NMR spectrum of the active lanthanum polymer chain exhibits a signal at 8.0 ppm ($OC(O)HBH_3$) and none at 4.8 ppm (OCH_2OBH_2), whereas it displays a ^{13}C NMR signal at 161.2 ($OC_{I2}(O)H$), thus highlighting the presence of the carbonyl and further supporting the absence of carbonyl reduction.

In the absence of carbonyl reduction by the adjacent BH_3 group in **2**, the stability toward borane elimination from **2** should be considered. Either the borane adduct is eliminated directly from **2** upon formation of **2′** (Scheme 5b), or it is eliminated upon deactivation of the living polymer **3** to form **4** (Scheme 5a). Unfortunately, evidence of BH_3 elimination from **2** to give $[Sm\{O(CH_2)_3OC(O)H\}_3]$, **2′**, could not be obtained. Indeed, in situ NMR analysis of the reaction of $[La(BH_4)_3(thf)_3]$ with eight equivalents of TMC remains inconclusive: the BH_3·THF or $-OC(O)HBH_3$ ^1H signals (which would appear within the same range (0–2 ppm)) are covered by the La–TMC oligomer peaks, whereas the two species **2** and **2′** would display similar ^{11}B NMR chemical shifts. Furthermore, we verified that reactions of the BH_3·THF adduct, formed eventually during the initiation process, with the incoming monomer or with the growing polymer chain are not observed, as reported previously.[50] In addition, the formate end group of methyl formate remains unaffected by the borane adduct. However, whatever the exact circumstances of BH_3·THF elimination, the whole process leads to a final polymer that always exhibits formate and hydroxyl chain ends, HO-PTMC-OC(O)H, **4**.

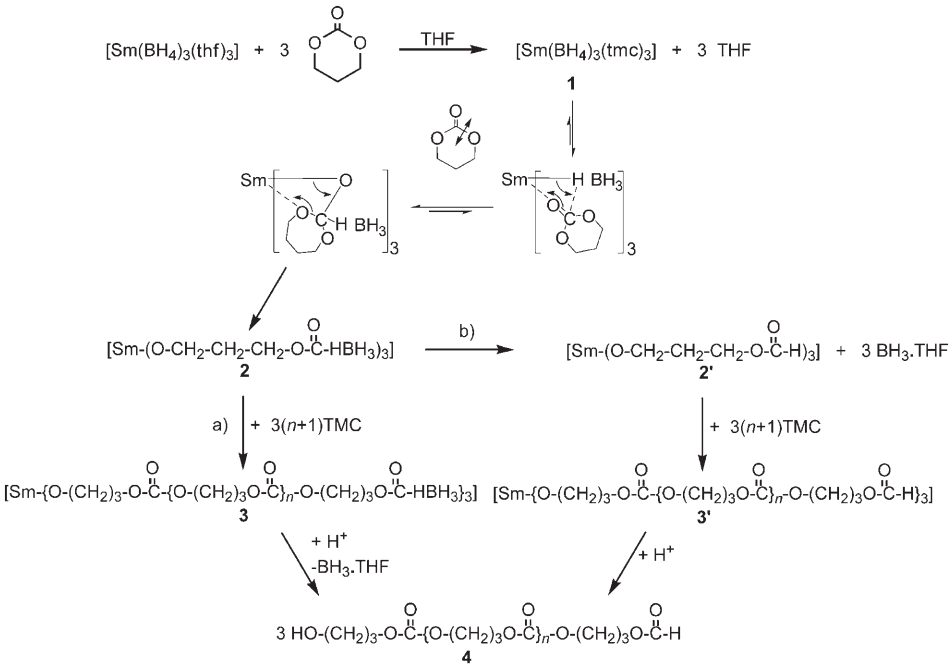

Scheme 5. Proposed mechanism for the polymerization of TMC initiated by $[Sm(BH_4)_3(thf)_3]$.

Consequently, the whole initiation step involves i) displacement of THF by the incoming TMC to form $[Sm(BH_4)_3(tmc)_3]$, **1**, ii) oxygen–acyl bond cleavage leading to $[Sm\{O(CH_2)_3OC(O)HBH_3\}_3]$, **2**, and eventually iii) borane elimination as the BH_3·THF adduct to give $[Sm\{O(CH_2)_3OC(O)H\}_3]$, **2′**. The real initiating complex in the polymerization of TMC is thus an alkoxide species, **2** or **2′**. Such an initiation mechanism is different from that proposed for the polymerization of CL initiated by the same initiator $[Sm(BH_4)_3(thf)_3]$, in that the carbonyl function –O–C(O)– of TMC is not reduced by the adjacent HBH_3 group, as was the carbonyl group –C(O)– of CL.[14,16]

Polymerization of TMC then proceeds within the samarium–oxygen bond of **2** or **2′** to give the active polymer $[Sm\{O(CH_2)_3OC(O)\{O(CH_2)_3OC(O)\}_nO(CH_2)_3OC(O)HBH_3\}_3]$, **3** or $[Sm\{O(CH_2)_3OC(O)\{O(CH_2)_3OC(O)\}_nO(CH_2)_3OC(O)H\}_3]$, **3′** (Scheme 5). Quenching the reaction induces the hydrolysis of this Sm–O-

(polymer) bond, resulting in the hydroxyl chain end of the final polymer **4**. The other polymer formate end group arises, either directly from $[Sm\{O(CH_2)_3OC(O)H\}_3]$, **2′**, or from the final $-C(O)HBH_3$ acidic hydrolysis of **3**, thereby eliminating BH_3 during this last step. The α,ω-telechelic polycarbonate can thus be formulated as HO-$(CH_2)_3OC(O)\{O(CH_2)_3OC(O)\}_nO(CH_2)_3OC(O)$H, HO-PTMC-OC(O)H, **4**. From all these results, the whole mechanism for the polymerization of TMC initiated by $[Sm(BH_4)_3(thf)_3]$, illustrated in Scheme 5, can be suggested.

The mechanism unveiled here thus represents the first pseudoanionic coordination-insertion type process fully detailed for the polymerization of a carbonate initiated by a rare-earth complex. This proposed mechanism is also different from the cationic process described for the polymerization of TMC initiated by rare-earth trishalides, which proceeds through an oxygen–alkyl bond scission of the monomer.[20] This is confirmed by the high concentration of ether segments, a characteristic typical of a cationic pathway, which is not observed in the present study.[49]

Copolymerization of TMC and CL initiated by $[Sm(BH_4)_3(thf)_3]$

Random copolymerization: Simultaneous additions of TMC and CL monomers to $[Sm(BH_4)_3(thf)_3]$ in THF or CH_2Cl_2 at ambient temperature allow the synthesis of random copolymers in high yields (Table 2). The random TMC–CL copolymers exhibit monomodal SEC traces. The molar-mass distribution values (average $\bar{M}_w/\bar{M}_n = 1.48$) remain below those reported previously for homoleptic halide or alkoxide rare-earth initiator (1.6,[31] 1.35–2.09,[23] 1.73–2.14,[22] 1.3–3.7[34]), suggesting a better control and a higher reactivity of this trisborohydride initiator. Only the monoalkoxide initiator (EA)Ln(OiPr) gives PTMC-*co*-PCL displaying narrower $\bar{M}_w/\bar{M}_n$ distributions (1.25–1.45), presumably as a result of the favourable influence of the diethyl acetoacetate surrounding ligand.[35] The experimental results indicate that both monomers display similar reactivity, however, according to NMR investigations, TMC would insert before CL during the initiation step.

^{1}H NMR spectra of PTMC-*co*-PCL exhibit both the hydroxyl ($\delta = 3.65$ ppm) and the formate ($\delta = 8.05$ ppm) chain end-functions, suggesting that TMC would coordinate and insert in the Sm–BH_4 bond before CL (Figure 7). Integration of the four signals at $\delta = 4.23$–4.05 ppm (H*a*, *1*, *2*, H*c*) allow the relative amounts of TMC–TMC, CL–CL, TMC–CL, and CL–TMC diad structures in the polymer to be evaluated as 63, 10, 8.5, and 18.5%, respectively, and peaks at 4.10 and 4.06 ppm provide evidence for the direct bonding between TMC and CL units.[23]

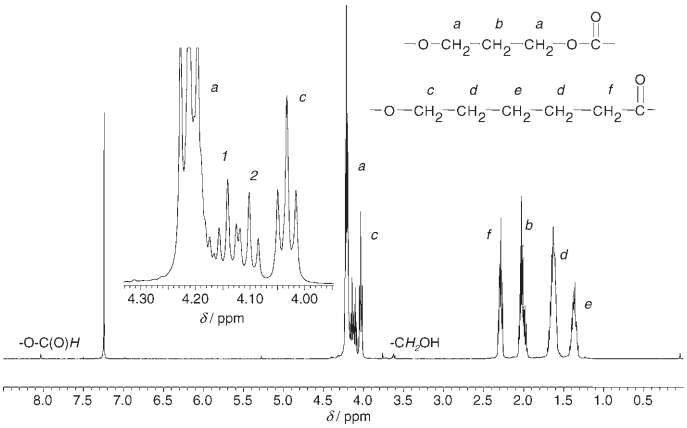

Figure 7. ^{1}H NMR spectrum in $CDCl_3$ of $PTMC_{52}$-*co*-PCL_{48} ($\bar{M}_{n(SEC)} = 8700\ g\,mol^{-1}$) synthesized from $[Sm(BH_4)_3(thf)_3]$.

Differential scanning calorimetry (DSC) analysis of $PTMC_{52}$-*co*-PCL_{48} reveals a glass transition temperature ($T_g = -35$ °C) intermediate between those of P(CL) (−60 °C) and P(TMC) (−15 °C) and a melting temperature ($T_m = 48$ °C) lower than that of PCL (60 °C), thereby supporting the random structure of the copolymers (Figure 8).

Block copolymerization: Sequential copolymerization of TMC with CL is carried out by introducing either TMC or CL first, resulting in copolymers of various chain end-functions (Scheme 6). The first monomer is added to $[Sm(BH_4)_3(thf)_3]$ and once fully converted, the comonomer is introduced. Copolymers of various compositions are obtained by varying the amount of monomers in the feed (Table 3). Reactions were performed in CH_2Cl_2 rather than in THF to avoid an undesired increase in viscosity of the reaction medium as observed previously during the synthesis of PCL from such borohydride initiators in THF.[14–17] The molar composition of the isolated copolymers (comp.$_{NMR}$), determined upon integrating the characteristic ^{1}H resonance of PTMC ($CH_2CH_2CH_2$, $\delta = 2.04$–1.98 ppm) and PCL ($CH_2C(O)$, $\delta = 2.30$–2.24 ppm), is in agreement with the

Table 2. Random copolymerization of TMC and CL initiated by $[Sm(BH_4)_3(thf)_3]$.

$[BH_4]_0$[a] [mmol L^{-1}]	$[TMC]_0$ [mmol L^{-1}]	$[CL]_0$ [mmol L^{-1}]	$[TMC]_0/[CL]_0$	Reaction time [min]	Solvent	Conv. TMC[b] [%]	Conv. CL[b] [%]	Comp.$_{theo}$ $[TMC]_0/[CL]_0$[c]	$\bar{M}_{n(theo)}$[d] [g mol^{-1}]	Comp.$_{NMR}$ $[TMC]_0/[CL]_0$[e]	$\bar{M}_{n(SEC)}$[f] [g mol^{-1}]	$\bar{M}_w/\bar{M}_n$[g]
11.47	280	1038	21/79	240	THF	96	88	22/78	11500	28/72	8400	1.51
17.69	1179	1127	51/49	180	CH_2Cl_2	98	98	51/49	13800	52/48	8700	1.56
10.4	700	644	52/48	240	THF	95	87	54/46	12700	56/44	8100	1.39
10.4	1120	265	81/19	240	THF	96	53	89/11	12100	91/9	8200	1.46

[a] $[BH_4]_0 = 3\,[Sm(BH_4)_3(thf)_3]_0$. [b] Determined by ^{1}H NMR analysis. [c] Theoretical composition of the copolymer determined from $[TMC]_0/[CL]_0$ taking into account the TMC and CL conversions. [d] Calculated from ($[TMC]_0/[BH_4]_0 \times 102 \times$ TMC conversion + $[CL]_0/[BH_4]_0 \times 114 \times$ CL conversion). [e] Composition of the precipitated copolymer determined from ^{1}H NMR analysis. [f] Determined by SEC ($\bar{M}_{n(SEC)} = \bar{M}_{n(SEC\ raw\ data)} \times 0.73 \times$ TMCcomp.$_{NMR}$ + $\bar{M}_{n(SEC\ raw\ data)} \times 0.56 \times$ CLcomp.$_{NMR}$). [g] Molar-mass distribution calculated from SEC chromatogram traces.

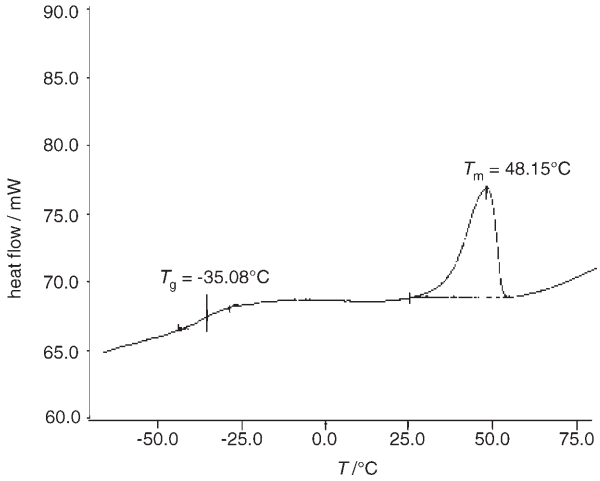

Figure 8. DSC of $PTMC_{52}$-*co*-PCL_{48}.

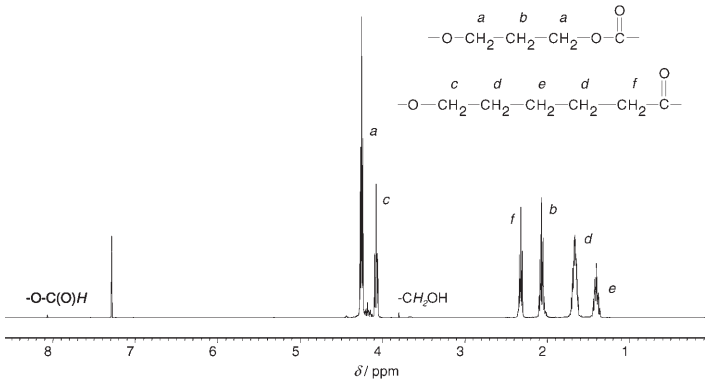

Figure 9. ^{1}H NMR spectrum in $CDCl_3$ of PCL_{45}-*b*-$PTMC_{55}$ ($\bar{M}_{n(SEC)}$ = 10150 g mol^{-1}) synthesized from $[Sm(BH_4)_3(thf)_3]$.

feed ratio ($[TMC]_0/[CL]_0$). Block copolymerizations with TMC monomer added first give copolymers with quite controlled features ($\bar{M}_n$ and $\bar{M}_w/\bar{M}_n$). Polymers with monomodal SEC curves and relatively narrow and similar molar-mass distributions (1.4–1.5) are obtained whatever the monomer composition and order of addition.

^{1}H NMR analysis of the copolymers allows the monomer that inserts first to be identified (Scheme 6). Indeed, initial polymerization of TMC induces the formation of two different PTMC-*b*-PCL chain ends, a hydroxyl (δ = 3.59 ppm) and a formate (δ = 7.99 ppm) (HO-PCL-*b*-PTMC-OC(O)H), whereas initial polymerization of CL gives a dihydroxy copolymer (HO-PTMC-*b*-PCL-OH) displaying only one type of end-function (δ = 3.61 ppm) (Figures 9 and 10).

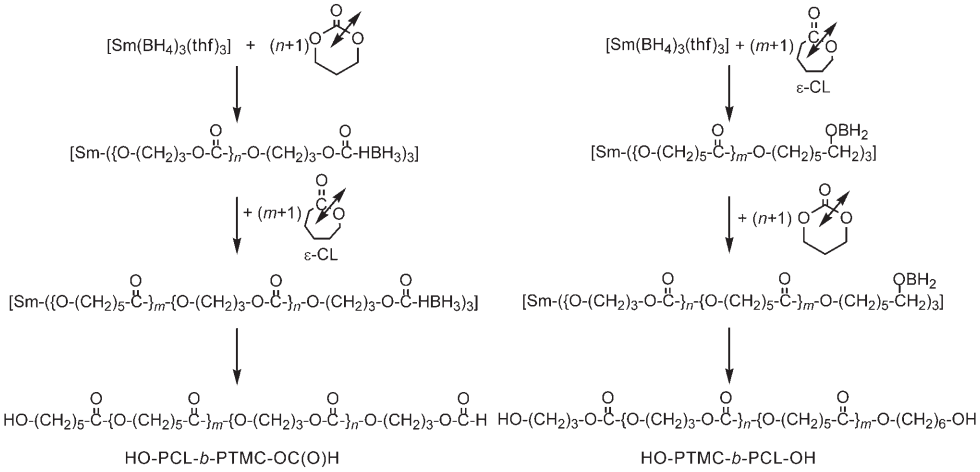

Scheme 6. Synthesis and chemical structure of PTMC/PCL block copolymers.

Table 3. Block copolymerization of TMC and CL initiated by $[Sm(BH_4)_3(thf)_3]$ in CH_2Cl_2.

$[BH_4]_0$[a] [mmol L^{-1}]	$[TMC]_0$ [mmol L^{-1}]	$[CL]_0$ [mmol L^{-1}]	$[TMC]_0/[CL]_0$	Order of monomer addition	Reaction time of each monomer [min]	Conv. TMC[b] [%]	Conv. CL[b] [%]	$Comp._{theo}$ $[TMC]_0/[CL]_0$[c]	$\bar{M}_{n(theo)}$[d] [g mol^{-1}]	$Comp._{NMR}$ $[TMC]_0/[CL]_0$[e]	$\bar{M}_{n(SEC)}$[f] [g mol^{-1}]	$\bar{M}_w/\bar{M}_n$[g]
24.3	1634	1002	62/38	TMC/CL	180/180	75	89	58/42	9300	55/45	8900	1.40
15.7	1129	752	60/40	TMC/CL	60/120	98	90	62/38	12100	57/43	9100	1.45
1.81	113	127	47/53	CL/TMC	30/120	79	81	46/54	11500	40/60	9400	1.43
1.83	113	123	49/51	CL/TMC	45/120	67	92	41/59	11300	42/58	11200	1.50

[a] $[BH_4]_0 = 3[Sm(BH_4)_3(thf)_3]_0$. [b] Determined by ^{1}H NMR analysis. [c] Theoretical composition of the copolymer determined from $[TMC]_0/[CL]_0$ taking into account the TMC and CL conversions. [d] Calculated from ($[TMC]_0/[BH_4]_0 \times 102 \times$ TMC conversion $+ [CL]_0/[BH_4]_0 \times 114 \times$ CL conversion). [e] Composition of the precipitated copolymer determined by ^{1}H NMR analysis. [f] Determined by SEC ($\bar{M}_{n(SEC)} = \bar{M}_{n(SEC\ raw\ data)} \times 0.73 \times TMCcomp._{NMR} + \bar{M}_{n(SEC\ raw\ data)} \times 0.56 \times CLcomp._{NMR}$). [g] Molar-mass distribution calculated from SEC chromatogram traces.

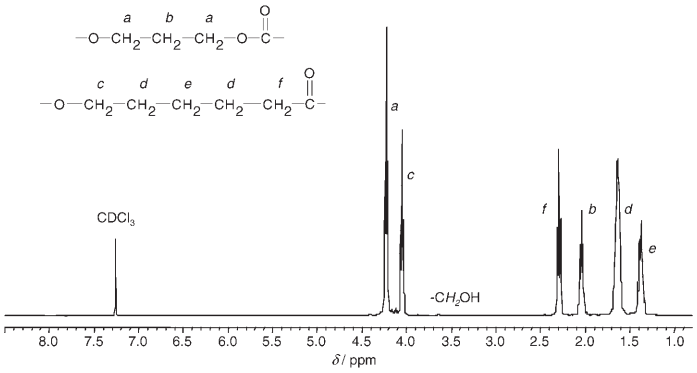

Figure 10. ^{1}H NMR spectrum in $CDCl_3$ of PCL_{60}-*b*-$PTMC_{40}$ ($\bar{M}_{n(SEC)}$ = 17400 g mol^{-1}) synthesized from $[Sm(BH_4)_3(thf)_3]$.

DSC thermograms of both copolymers exhibit two glass transitions corresponding to each block and a melting temperature arising from the PCL unit, as illustrated with HO-PCL_{60}-*b*-$PTMC_{40}$-OH (T_g = −60 °C, −16 °C, T_m = 64 °C; Figure 11). These data confirm the block structure of the copolymers.

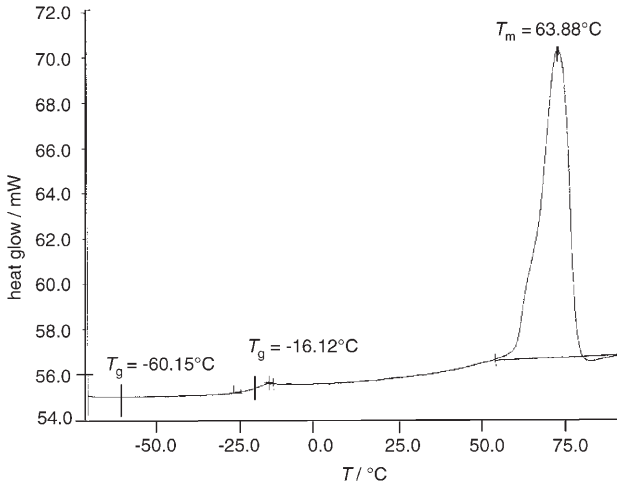

Figure 11. DSC of PCL_{60}-*b*-$PTMC_{40}$.

Conclusions

The rare-earth borohydride complex $[Sm(BH_4)_3(thf)_3]$ is an efficient initiator for the controlled ROP of TMC at ambient temperature to form α-formate,ω-hydroxy telechelic poly(trimethylenecarbonate). Synthesis of such a formate end-functionalized polyester, reported here for the first time, relies on the intrinsic reactivity of the samarium-bound borohydride ligand, which does not reduce the −O−C(O)− carbonyl and which is eliminated as BH_3·THF. Mechanistic insights are gained from thorough NMR analyses, especially of the polycarbonate chain ends.

The borohydride complex $[Sm(BH_4)_3(thf)_3]$ also represents a new and efficient rare-earth initiator active in TMC/CL random and block copolymerization, allowing the synthesis of either α,ω-dihydroxy or α-formate,ω-hydroxy telechelic PTMC–PCL copolymers. Although the order of introduction of the comonomers dictates the copolymer chain ends, it does not affect the block copolymerization, which proceeds regardless. The borohydride nature of the initiator has again a direct impact on the polymer chain end, and thereby allows the synthesis of PTMC–PCL copolymers with an unprecedented formate end-function, thus opening the route to new tailor-made biomaterials.

Experimental Section

Materials: Due to the sensitivity of the rare-earth complexes, all manipulations were performed under inert atmosphere (argon, <3 ppm of O_2) using standard Schlenk, vacuum-line, and glove-box techniques. Solvents were dried thoroughly and were deoxygenated by standard methods and distilled before use.[15] CD_2Cl_2 and $CDCl_3$ were dried over a mixture of 3- and 4-Å molecular sieves. ε-Caprolactone (ε-CL, Lancaster) was dried successively over CaH_2 (for at least one week) and 4,4′-methylenebis(phenylisocyanate). Trimethylene carbonate (TMC, 1,3-dioxane-2-one, Labso Chimie Fine) was dissolved in THF and was stirred over CaH_2 for two days before being filtrated and finally dried. Diethylcarbonate (DEC, $CH_3CH_2OC(O)OCH_2CH_3$, Aldrich) was dried over CaH_2: ^{1}H NMR ($CDCl_3$): δ = 4.12 (q, 4H; CH_2), 1.24 ppm (t, 6H; CH_3); ^{13}C{^{1}H} NMR ($CDCl_3$): δ = 154.7 (O*C*(O)O), 62.7 (*C*H_2), 14.0 ppm (*C*H_3) (Figure 3). $[Sm(BH_4)_3(thf)_3]$ and $[La(BH_4)_3(thf)_3]$ were synthesized from $SmCl_3$ or $LaCl_3$ (Aldrich) by following the literature procedure, and were then characterized accordingly.[14,40,41] $[Sm(BH_4)_3(thf)_3]$: ^{1}H NMR ($CDCl_3$): δ = 4.23 (s, $w_{1/2}$ = 20 Hz, 12H; THF), 2.22 (s, $w_{1/2}$ = 15 Hz, 12H; THF), −10.6 ppm (br q, $w_{1/2}$ = 430 Hz, 12H; BH_4); ^{13}C{^{1}H} NMR (CD_2Cl_2): δ = 74.8 (s; THF), 25.6 ppm (s; THF) (Figure 3). $[La(BH_4)_3(thf)_3]$: ^{1}H NMR ($CDCl_3$): δ = 1.16 (br q, $w_{1/2}$ = 280 Hz, J_{BH} = 80 Hz, 12H; BH_4), 4.18 and 2.00 ppm (t, 12H; t, 12H; THF). All other reagents were available commercially (Aldrich).

Instrumentation and measurements: ^{1}H (400 MHz) and ^{13}C (100 MHz) NMR spectra were recorded in CD_2Cl_2 or $CDCl_3$ by using a Bruker Avance DPX 400 at 23 °C and were referenced internally by using the residual ^{1}H and ^{13}C solvent resonance relative to tetramethylsilane (δ = 0). Average molar mass ($\bar{M}_n$) and molar-mass distribution ($\bar{M}_w/\bar{M}_n$) values were determined from chromatogram traces recorded by SEC in THF at 20 °C (flow rate 1.0 mL min^{-1}) by using a Varian apparatus equipped with a refractive index detector and three TSK HXL columns G2000, 3000, 4000. The polymer samples were dissolved in THF (2 mg mL^{-1}). The elution curves were calibrated with polystyrene standards and raw values ($\bar{M}_{n(SEC\ raw\ data)}$) were thus obtained. $\bar{M}_{n(SEC)}$ values of PTMC were calculated by using the correction coefficient X ($\bar{M}_{n(SEC)} = \bar{M}_{n(SEC\ raw\ data)} \times X$). The values of this correcting factor X were determined upon comparing the $\bar{M}_{n(SEC\ raw\ data)}$ values to those obtained from either MALDI-TOF (for $\bar{M}_{n(SEC\ raw\ data)} < 5000$ g mol^{-1}) or viscosimetry measurements (for $\bar{M}_{n(SEC\ raw\ data)} > 10000$ g mol^{-1}), for the same polymers. The average values of the coefficient determined are X = 0.57 for $\bar{M}_{n(SEC\ raw\ data)} < 5000$ g mol^{-1} and X = 0.88 for $\bar{M}_{n(SEC\ raw\ data)} > 10000$ g mol^{-1}. Comparison of PTMC molar masses determined from SEC and MALDI-TOF or viscosimetry measurements are reported as Supporting Information. Within the range $5000 < \bar{M}_{n(SEC\ raw\ data)} < 10000$ g mol^{-1}, an average value between these two data was applied (X = 0.73). Actual PTMC molar-mass values ($\bar{M}_{n(SEC)}$) were then subsequently conveniently derived from molar-mass values calibrated with polystyrene standards $\bar{M}_{n(SEC\ raw\ data)}$ according to $\bar{M}_{n(SEC)} = \bar{M}_{n(SEC\ raw\ data)} \times 0.88/0.73/0.57$. $\bar{M}_{n(SEC)}$ values of PCL were calculated by using the correction coefficient reported previously (unique value for all molar-mass polymers; $\bar{M}_{n(SEC)} = \bar{M}_{n(SEC\ raw\ data)} \times 0.56$).[10,11,14–16,36f] Intrinsic viscosity values of PTMCs with molar mass >10000 g mol^{-1} were measured by using an automated Ubelhodde viscometer in THF at 30 °C. The viscosity average molar masses ($\bar{M}_{(visco)}$) of PTMCs were then calculated according to the Mark–Houwink equation determined for PTMC in THF

at 30 °C, $[\eta]$ $(dL\,g^{-1}) = 2.77 \times 10^{-4}\,\bar{M}_{(visco)}^{0.677}$.[20,36f,h,51–52] PTMC molar masses $< 5000\ g\,mol^{-1}$ were determined by MALDI-TOF MS analyses. MALDI-TOF MS experiments were performed by the CESAMO (Bordeaux, France) by using a Reflex apparatus (Bruker) equipped with a pulsed N_2 laser (337 nm, 4-ns pulse width) and time-delayed extracted ion source. Spectra were recorded in the positive-ion mode by using the reflectron mode and an accelerating voltage of 20 kV. Polymer samples were dissolved in THF ($10\ mg\,mL^{-1}$), and solutions of ditranol/THF ($10\ mg\,mL^{-1}$) and NaI/MeOH ($10\ mg\,mL^{-1}$) were prepared as matrix and cation source, respectively. These three solutions were then mixed in a 1:10:1 volume ratio, respectively, deposited on the sample target, and then air-dried.

The monomer conversions were calculated from ^{1}H NMR spectra of the crude polymer sample from the integration (Int.) ratio Int.P(TMC)/[Int.P(TMC) + Int.(TMC)] by using the methylene group ($CH_2CH_2CH_2$, $\delta = 4.21$ ppm or $CH_2CH_2CH_2$, $\delta = 2.02$ ppm) for TMC and from the integration ratio Int.P(ε-CL)/[Int.P(ε-CL) + Int.(ε-CL)] by using the methylene group in the α-position of the carbonyl ($CH_2C(O)$, $\delta =$ 2.4–2.2 ppm) for CL.

Differential scanning calorimetry (DSC) analyses were performed by using a Perkin–Elmer DSC-7 apparatus under nitrogen, within a temperature range of −100 °C to 100 °C with a heating rate of 10 °C min^{-1}.

Reaction of $[Sm(BH_4)_3(thf)_3]$ with diethylcarbonate (DEC): $[Sm(BH_4)_3(thf)_3]$ (6.3 mg, 15.3 μmol) and DEC (5.6 μL, 46.2 μmol) were dissolved in $CDCl_3$ in an NMR tube. The tube was then placed in an ultrasound bath at RT for 5 min. Subsequent analysis showed the formation of $[Sm(BH_4)_3(dec)_3]$ along with the release of THF. ^{1}H NMR ($CDCl_3$): $\delta = 4.22$ (q, 4H; CH_2), 3.81 (s, $w_{1/2} = 15$ Hz, 12H; THF), 1.94 (s, $w_{1/2} = 15$ Hz, 12H; THF), 1.31 (t, 6H; CH_3), −7.2 ppm (br q, $w_{1/2} = 310$ Hz, 12H; BH_4) (Figure 6); ^{13}C{^{1}H} NMR ($CDCl_3$): $\delta = 155.2$ ($OC(O)O$), 71.0 (THF), 64.7 (CH_2), 25.4 (THF), 14.3 ppm (CH_3).

Stoichiometric reaction of $[Sm(BH_4)_3(thf)_3]$ with TMC: $[Sm(BH_4)_3(thf)_3]$ (82 mg, 200 μmol) and TMC (61 mg, 600 μmol) were placed together in a reaction flask and CH_2Cl_2 was added. The clear, colorless solution was stirred for 120 min. After filtration and drying, $[Sm(BH_4)_3(tmc)_3]$, **1**, was recovered as a white powder (97% yield). IR (Nujol): $\tilde{\nu} = 2727$ (s; C−H), 2425 (m), 2360 (m), 2285 (m), 2221 (m), 2165 (m; B−H), 1750 (w; C=O), 1462 (s), 1376 (s), 1346 (s), 1284 (s), 1262 (s), 1082 cm^{-1} (vs br). No THF (free or Sm-coordinated) was observed.

Reaction of BH_3·THF with TMC, PTMC, $CH_3OC(O)H$: BH_3·THF was placed in an NMR tube and was concentrated. The second reagent was added in stoichiometric amount and the reactions were monitored by performing NMR spectroscopy.

Reaction of $[La(BH_4)_3(thf)_3]$ with TMC: $[La(BH_4)_3(thf)_3]$ (2.6 mg, 6.5 μmol) and TMC (8 equiv, 15.9 mg, 156 μmol) were dissolved in CD_2Cl_2 in an NMR tube. The tube was then placed in an ultrasound bath at RT for 5 min. Subsequent analysis showed the formation of $[La\{O(CH_2)_3OC(O)\}_nO(CH_2)_3OC(O)H/BH_3]$, along with the release of THF (the BH_3 signal most likely overlapped with those of the polymer). ^{1}H NMR (CD_2Cl_2): $\delta = 8.01$ (s, 1H; OC(O)*Hj*), 4.23 ppm (t, J(H,H) = 6.1 Hz, (4*n*+6)H; $CHd_2CH_2CHf_2$, $CHg_2CH_2CHi_2OC(O)H$, $LaOCH_2CH_2CHc_2OC(O)$-), 3.74 (m, 2H; $LaOCHa_2$), 2.04 (t, J(H,H) = 6.2 Hz, (2*n*+2)H; $CH_2CHe_2CH_2$, $CH_2CHh_2CH_2OC(O)H$)), 1.80 ppm (m, 2H; $LaOCH_2CHb_2CH_2OC(O)$-); ^{13}C{^{1}H} NMR (CD_2Cl_2): $\delta = 161.2$ ($OC_{12}(O)H$), 155.7, 155.3 ($OC_{4,8}(O)O$), 66.0, 60.6 ($CH_2C_{3,9,11}H_2OC(O)O$), 64.7 ($OC(O)OC_5H_2CH_2C_7H_2OC(O)O$), 59.6 ($HOC_1H_2$), 31.0, 27.4 ($CH_2C_{10}H_2CH_2OC(O)H$, $HOCH_2C_2H_2CH_2$), 28.5 ($OC(O)OCH_2C_6H_2CH_2OC(O)$), 25.9 ppm (THF).

Typical TMC homopolymerization: A solution of TMC (500 mg, 4.9 mmol) in THF (2 mL) was added under vacuum with a burette to a stirred solution of $[Sm(BH_4)_3(thf)_3]$ (7.8 mg, 19.0 μmol) in CH_2Cl_2 or THF (2 mL) at 21 °C. The suspension was stirred for 90 min and the polymerization was stopped upon addition of an acetic acid solution (16.5×10^{-3} mol L^{-1} in toluene, 1 mL). The resulting mixture was then dried and the monomer conversion was determined. The crude polymer sample was then dissolved in CH_2Cl_2, precipitated in cold MeOH, filtered, and dried to afford pure PTMC. The resulting PTMC were then characterized by ^{1}H and ^{13}C NMR, SEC, viscosimetry, or MALDI-TOF analyses. ^{1}H NMR ($CDCl_3$): $\delta = 8.03$ (s, 1H; OC(O)*Hj*), 4.27 (m shoulder of signal at 4.21) 4.21 (t, J(H,H) = 6.0 Hz, (4*n*+6)H; $CHd_2CH_2CHf_2$, $CHg_2CH_2CHi_2OC(O)H$, $HOCH_2CH_2CHc_2OC(O)$), 3.71 (t, 2H; $HOCHa_2$), 2.02 (t, J(H,H) = 6.2 Hz, (2*n*+2)H; $CH_2CHe_2CH_2$, $CH_2CHh_2CH_2OC(O)H$), 1.89 ppm (quint., J(H,H) = 6.7 Hz, 2H; $HOCH_2CHb_2CH_2OC(O)$). The broad singlet at 1.60 ppm results from the presence in the sample of H_2O traces (hard to remove),[23,36c] as monitored by ^{1}H NMR, showing an increase of this signal upon addition of 10 μL of H_2O to a PTMC ($\bar{M}_n$(SEC) = 2950 g mol^{-1}, 15 mg, 5 μmol) sample in $CDCl_3$. Impurities signals (*) at 3.76 and 1.24 ppm are uncoupled in the COSY spectrum. ^{13}C NMR ($CDCl_3$): $\delta = 161.8$ ($OC12(O)H$), 156.2, 155.8 ($OC4,8(O)O$), 66.0, 61.2 ($CH_2C3,9,11H_2OC(O)O$), 65.2 ($OC(O)OC5H_2CH_2C7H_2OC(O)O$), 59.9 ($HOC1H_2$), 32.6 ($HOCH_2C2H_2CH_2$), 29.0 ($OC(O)OCH_2C6H_2CH_2OC(O)$), 28.9 ppm ($CH_2C10H_2CH_2OC(O)H$).

Random TMC–CL copolymerization: A THF or CH_2Cl_2 (5.8 mL) solution of both TMC (800 mg; 7.8 mmol) and CL (206 μL; 1.95 mmol) was added to a stirred solution of $[Sm(BH_4)_3(thf)_3]$ (10 mg; 24.2 μmol) in THF or CH_2Cl_2 (1 mL) at 21 °C. The polymerization was then stopped after 3–4 h upon addition of an acetic acid solution (16.5×10^{-3} mol L^{-1} in toluene, 1 mL) and then dried. After determination of the monomer conversion by ^{1}H NMR spectroscopy, the resulting mixture was dissolved in CH_2Cl_2, precipitated in cold methanol, filtered, and finally dried to afford the copolymer PTMC-*co*-PCL. ^{1}H NMR ($CDCl_3$): $\delta = 8.05$ (s; -OC(O)*H*), 4.23 (t; -$OCH_2CH_2CH_2OC(O)$-), 4.10 (m; -$OC(O)CH_2$-$(CH_2)_4C(O)$-, TMC–CL diad), 4.06 (m; -$CH_2C(O)OCH_2(CH_2)_2OC(O)$-, CL–TMC diad), 3.99 (t; -$OCH_2(CH_2)_4C(O)$-), 3.65 (t; $HOCH_2$), 2.30 (m; -$(CH_2)_4CH_2C(O)$-), 2.04 (m; -$OCH_2CH_2CH_2OC(O)$-), 1.65 (m; -$OCH_2CH_2(CH_2)_3C(O)$-), 1.38 ppm (m; -$(CH_2)_2CH_2(CH_2)_2C(O)$-).

Block TMC–CL copolymerization

Addition of CL first: CL (500 μL; 4.9 mmol) in CH_2Cl_2 (2.0 mL) was added under vacuum by using a burette onto a stirred solution of $[Sm(BH_4)_3(thf)_3]$ (10 mg; 24.2 μmol) in CH_2Cl_2 (1.0 mL) at 21 °C. After an appropriate reaction time (30–45 min), TMC (500 mg; 4.92 mmol) in CH_2Cl_2 (1 mL) was added similarly and the polymerization was allowed to proceed for 2 h. Hydrolysis of the reaction mixture, precipitation, and drying of the copolymer were performed as described above for random copolymer synthesis. ^{1}H NMR ($CDCl_3$): $\delta = 4.22$ (t; -$OCH_2CH_2CH_2OC(O)$), 4.06 (t; -$OCH_2(CH_2)_4C(O)$-); 3.61 (t; $HOCH_2$), 2.30 (t; -$CH_2C(O)$), 2.04 (m; -$OCH_2CH_2CH_2OC(O)$-), 1.62 (m; -$OCH_2CH_2(CH_2)_3C(O)$-), 1.37 ppm (m; -$(CH_2)_2CH_2(CH_2)_2C(O)$-).

Addition of TMC first: TMC (500 mg; 4.9 mmol) in CH_2Cl_2 (2.0 mL) was added under vacuum by using a burette onto a stirred solution of $[Sm(BH_4)_3(thf)_3]$ (10 mg; 24.2 μmol) in CH_2Cl_2 (1 mL) at 21 °C. After an appropriate reaction time (60–180 min), CL (500 μL; 4.9 mmol) in CH_2Cl_2 (1.0 mL) was added similarly and the polymerization was allowed to proceed over 120–180 min. Hydrolysis of the reaction mixture, precipitation, and drying of the copolymer were performed as described above for random copolymer synthesis. ^{1}H NMR ($CDCl_3$): $\delta = 7.99$ (s; -OC(O)*H*), 4.17 (t; -$OCH_2CH_2CH_2OC(O)$), 3.99 (t; -$OCH_2(CH_2)_4C(O)$-); 3.59 (t; $HOCH_2$), 2.24 (t; -$(CH_2)_4CH_2C(O)$-), 1.98 (q; -$OCH_2CH_2CH_2OC(O)$-), 1.56 (m; -$OCH_2CH_2(CH_2)_3C(O)$-), 1.32 ppm (m; -$(CH_2)_2CH_2(CH_2)_2C(O)$-).

[1] Z. Hou, Y. Wakatsuki, *Coord. Chem. Rev.* **2002**, *231*, 1–22.
[2] S. Agarwal, C. Mast, K. Dehnicke, A. Greiner, *Macromol. Rapid Commun.* **2000**, *21*, 195–212.
[3] H. Yasuda, *Prog. Polym. Sci.* **2000**, *25*, 573–626.
[4] A.-C. Albertsson, I. K. Varma, *Adv. Polym. Sci.* **2002**, *157*, 1–40.
[5] K. M. Stridsberg, M. Ryner, A.-C. Albertsson *Adv. Polym. Sci.* **2002**, *157*, 42–65.
[6] A. Amgoune, C. Thomas, S. Ilinca, T. Roisnel, J.-F. Carpentier, *Angew. Chem.* **2006**, *118*, 2848–2850; *Angew. Chem. Int. Ed.* **2006**, *45*, 2782–2784.
[7] A. Amgoune, C. Thomas, T. Roisnel, J.-F. Carpentier, *Chem. Eur. J.* **2006**, *12*, 169–179.
[8] M. Vert, *Biomacromolecules* **2005**, *6*, 538–546.

[9] A.-C. Albertsson, I. K. Varma, *Biomacromolecules* **2003**, *4*, 1466–1486.
[10] M. Save, A. Soum, *Macromol. Chem. Phys.* **2002**, *203*, 2591–2603.
[11] M. Save, M. Schappacher, A. Soum, *Macromol. Chem. Phys.* **2002**, *203*, 889–899.
[12] S. Caillol, S. Lecommandoux, A.-F. Mingotaud, M. Schappacher, A. Soum, N. Bryson, R. Meyrueix, *Macromolecules* **2003**, *36*, 1118–1124.
[13] M. Schappacher, A. Soum, S. M. Guillaume, *Biomacromolecules* **2006**, *7*, 1373–1379.
[14] S. M. Guillaume, M. Schappacher, A. Soum, *Macromolecules* **2003**, *36*, 54–60.
[15] I. Palard, A. Soum, S. M. Guillaume, *Chem. Eur. J.* **2004**, *10*, 4054–4062.
[16] I. Palard, A. Soum, S. M. Guillaume, *Macromolecules* **2005**, *38*, 6888–6894.
[17] I. Palard, M. Schappacher, A. Soum, S. M. Guillaume, *Polym. Int.* **2006**, *55*, 1132–1137.
[18] S. Agarwal, M. Puchner, *Eur. Polym. J.* **2002**, *38*, 2365–2371.
[19] L. Zhou, Y. Yao, Y. Zhang, M. Xue, J. Chen, Q. Shen, *Eur. J. Inorg. Chem.* **2004**, 2167–2172.
[20] Y. Shen, Z. Shen, Y. Zhang, Q. Hang, *J. Polym. Sci. Part A* **1997**, *35*, 1339–1352.
[21] J. Ling, Z. Shen *Macromol. Chem. Phys.* **2002**, *203*, 735–738.
[22] L. Zhou, H. Sun, J. Chen, Y. Yao, Q. Shen, *J. Polym. Sci. Part A* **2005**, *43*, 1778–1786.
[23] J. Ling, W. Zhu, Z. Shen, *Macromolecules* **2004**, *37*, 758–763.
[24] H. Li, Y. Yao, C. Yao, H. Sheng, Q. Shen, *J. Polym. Sci. Part A* **2005**, *43*, 1312–1316.
[25] H. Yasuda, M.-S. Aludin, N. Kitamura, M. Tanabe, H. Sirahama, *Macromolecules* **1999**, *32*, 6047–6057.
[26] W. J. Evans, H. Katsumata, *Macromolecules* **1994**, *27*, 4011–4013.
[27] J. Ling, Z. Shen, Q. Huang, *Macromolecules* **2001**, *34*, 7613–7616.
[28] S. Agarwal, N. Naumann, X. Xie, *Macromolecules* **2002**, *35*, 7713–7717.
[29] H. Shirahama, A. Kanetani, H. Yasuda, *Polym. J.* **2000**, *32*, 280–286.
[30] C. Yu, ; L. Zhang, Z. L. Shen, *J. Mol. Catal. A* **2004**, *212*, 365–369.
[31] M. Schappacher, T. Fabre, A.-F. Mingotaud, A. Soum, *Biomaterials* **2001**, *22*, 2849–2855.
[32] Y. Shen, Z. Shen, Y. Zhang, Q. Huang, L. Shen, H. Yuan, *J. Appl. Polym. Sci.* **1997**, *64*, 2131–2139.
[33] T. Fabre, M. Schappacher, R. Bareille, B. Dupuy, A. Soum, J. Bertrand-Barat, C. Baquey, *Biomaterials* **2001**, *22*, 2951–2958.
[34] A. P. Pêgo, Z. Zhong, P. J. Dijkstra, D. W. Grijpma, J. Feijen, *Macromol. Chem. Phys.* **2003**, *204*, 747–754.
[35] Y. Shen, Z. Shen, Y. Zhang, K. Yao, *Macromolecules* **1996**, *29*, 8289–8295.
[36] PCL–PTMC copolymers were also prepared from other transition-metal compounds, such as tin[22] a) H. R. Kricheldorf, A. Stricker, *Macromol. Chem. Phys.* **1999**, *200*, 1726–1733; b) Y. T. Jia, H. Y. Kim, J. Gong, D. R. Lee, B. Ding, N. Bhattarai, *Polym. Int.* **2004**, *53*, 312–319; c) D. J. Darensbourg, P. Ganguly, D. Billodeaux, *Macromolecules* **2005**, *38*, 5406–5410; d) A. P. Pêgo, A. A. Poot, D. W. Grijpma, J. Feijen, *Macromol. Biosci.* **2002**, *2*, 411–419; e) J.-T. Hong, N.-S. CHO, H.-S. Yoon, T.-H. Kim, D.-H. Lee, W.-G. Kim, *J. Polym. Sci. Part A* **2005**, *43*, 2790–2799; bismuth f) H. R. Kricheldorf, S. Rost, *Macromolecules* **2005**, *38*, 8220–8226; zinc g) A. C. Albertsson, M. Eklund, *J. Polym. Sci. Part A* **1994**, *32*, 265–279; h) P. Dobrzynski, M. Pastusiak, M. Bero, *J. Polym. Sci. Part A* **2005**, *43*, 1913–1922; and aluminum i) M. Baiardo, C. A. Giovanni, *Macromol. Chem. Phys.* **2001**, *202*, 2509–2517.
[37] C. Tsutsumi, K. Yamamoto, A. Ichimaru, M. Nodono, K. Nakagawa, H. J. Yasuda, *Polym. Sci.* **2003**, 3572–3588.
[38] Q. Huang, Z. Shen, Y. Zhang, Y. Shen, L. Shen, H. Yuan, *Polym. J.* **1998**, *30*, 168–170.
[39] D. Pospiech, H. Komber, D. Jehnichen, L. Häussler, K. Eckstein, H. Scheibner, A. Janke, H. R. Kricheldorf, O. Petermann, *Biomacromolecules* **2005**, *6*, 439–446.
[40] S. M. Cendrowski-Guillaume, G. Le Gland, M. Nierlich, M. Ephritikhine, *Organometallics* **2000**, *19*, 5654–5660.
[41] S. M. Cendrowski-Guillaume, M. Nierlich, M. Lance, M. Ephritikhine, *Organometallics* **1998**, *17*, 786–788.
[42] U. Mirsaidov, I. B. Shaimuradov, M. Khikmatov, *Russ. J. Inorg. Chem.* **1986**, *31*, 753–754.
[43] S. M. Cendrowski-Guillaume, M. Nierlich, M. Ephritikhine, *Eur. J. Inorg. Chem.* **2001**, 1495–1498.
[44] S. M. Cendrowski-Guillaume, G. Le Gland, M. Lance, M. Nierlich, M. Ephritikhine, *C. R. Acad. Sci. Ser. IIc* **2002**, *5*, 73–80.
[45] The molar masses found in the literature for homoPTMCs synthesized from rare-earth initiating complexes are only virtual values (refs. [18-23]). Indeed, these data were determined relative to polystyrene standards by SEC without using any correction factor. Molar masses, reported from intrinsic viscosity measurements, for PTMC prepared from $LnCl_3$ did not, however, match the theoretical values. Molar-mass-distribution values obtained in the present study remain much lower than those published previously for PTMC prepared from rare-earth initiators (1.4–2.45) (refs. [18-23]).
[46] T. Ariga, T. Takara, T. Endo, *J. Polym. Sci. Part A* **1993**, *31*, 581–584.
[47] M. Ephritikhine, *Chem. Rev.* **1997**, *97*, 2193–2242.
[48] H. R. Kricheldorf, B. Weegen-Schulz, *Makromol. Chem. Rapid Commun.* **1993**, *14*, 405–411.
[49] H. R. Kricheldorf, J. Jenssen, Z. K. Saunders, *Makromol. Chem.* **1991**, *192*, 2391–2399.
[50] C. F. Lane, *Chem. Rev.* **1976**, *76*, 773–799.
[51] K. J. Zhu, R. W. Hendren, C. G. Pitt, *Macromolecules* **1991**, *24*, 1736–1740.
[52] H. R. Kricheldorf, A. Stricker, Z. Gomurashvili, *Macromol. Chem. Phys.* **2001**, *202*, 413–420.

Received: June 15, 2006
Published online: November 13, 2006

